Influence of intermittency on quantum spectra

1992 J. Phys. A: Math. Gen. 25 6265

(http://iopscience.iop.org/0305-4470/25/23/022)

J. Phys. A: Math. Gen. 25 (1992) 6265–6282. Printed in the UK

Influence of intermittency on quantum spectra

Per Dahlqvist

Mechanics Department, Royal Institue of Technology, S-100 44 Stockholm, Sweden

Received 1 May 1992

Abstract. Bound chaotic systems typically exhibit intermittency. Some semiclassical properties of intermittency are studied. The *hyperbola billiard* and the x^2y^2 model are used as strongly intermittent model systems. The almost integrable motion in the *arms* of the potential may be treated in the adiabatic approximation. The corresponding adiabatic Hamiltonian may be semiclassically quantized, yielding surprisingly good agreement for the hyperbola billiard. It is then demonstrated, by means of the semiclassical trace formula, how this result may be related to families of periodic orbit exclusively exploring the potential arms. It is discussed how this result implies an integrable component in the spectrum. Possible implications for the resummation problem of the trace formula, as well as for the statistical properties of energy levels, are discussed.

1. Introduction

By intermittency in a dynamical system we mean motion that alternates between chaotic and regular behaviour. Subregions in phase space associated with (nearly) integrable motion may be found in almost all types of dynamical systems and maps. In a generic Hamiltonian system, phase space is divided into regions with quasiperiodic motion, and regions with chaotic behaviour. Trajectories in the border between these regions will show intermittent behaviour. Periodic orbits in the layer between KAM surfaces will then have Liapunov exponents tending to zero as their periods go to infinity [1], which is a typical signal of intermittency.

Even strongly chaotic systems may exhibit intermittency. In, for example, the stadium billiard [2, 3] this is associated with the integrable subregion of the phase space corresponding to bouncing between the two straight lines connecting the semicircles. Note that this integrable subregion does not imply any quasiperiodic motion. All closed orbits have been scattered in the semicircles. The system has positive entropy and all periodic orbits will be unstable with one exception, the (degenerate) periodic orbit between the two straight sections has marginal stability. Sinai's billiard [4] is quite similar in this respect.

A particle scattering in the enclosure between three (or more) touching circular disks will also show intermittent behaviour, since the motion is almost integrable close to where the disks touch.

Generally, no bound system seems to provide hyperbolic (or axiom A) properties. Any Hamiltonian system may be represented by a map by means of a Poincaré surface of section. If the system is open, it is quite possible to realize a Smale horsehoe structure for the map with a well defined, complete symbolic dynamics as well as hyperbolicity, as in the scattering system consisting of three sufficiently spaced circular disks.

But if, on the other hand, the system is bound, a phase-space region will now be mapped onto itself. Assuming reasonable continuity conditions it will clearly be very difficult, or even impossible, to preserve hyperbolicity over the entire phase-space region and completeness of the symbolic dynamics; the hyperbolicity of the baker's map is possible because of a severe discontinuity.

In a phase space with periodic boundary conditions it is quite possible to define a hyperbolic system. The cat map [5] is continuous on the torus and is indeed hyperbolic. It is even possible to define smooth Hamiltonians on the 2-torus with ergodic flow [6]. These systems are entirely different, both classically and quantum mechanically, from the systems discussed in this paper and will be omitted from the discussion. We will also remain inside Euclidean space throughout this article.

This unavoidable presence of intermittency in bound systems is important from several points of view. On the classical level, intermittency may imply power-law corrections for the exponential decay of resonances [3, 7]. An intermittent system, with otherwise strong chaotic properties, is not structurally stable, as is the case with axiom-A systems. In a smooth bound system or, equivalently, in a smooth map, this means that small stable islands in phase space will normally exist [8], no matter how strongly chaotic the system is. In [9] it is shown how such small islands influence the decay of resonances, namely in the same way as intermittency does.

There has recently been much work devoted to the study of the quantum mechanics of systems exhibiting chaos on the classical level, for a review see [10]. Statistical studies of the set of quantum eigenvalues have been made, and for bound chaotic systems with time reversal symmetry, the level statistics have been conjectured [11] to agree with the Gaussian orthogonal ensemble (GOE). The level spacing distribution generally agrees well with the one given by GOE, but for other statistical measures, such as spectral rigidity, there is considerable disagreement [12, 13]. The understanding of these results from a semiclassical viewpoint is fragmentary. It is evident that the omnipresence of intermittency might be highly relevant in such a discussion.

It is also interesting to note that a small island of stability in a phase space corresponds to a regular part of the quantum spectrum [14, 15]. Due to the close connection between intermittency and these small stable islands it is natural to expect a regular component of the spectrum even in an arbitrary ergodic, but intermittent, system (e.g. billiard). Will this mean deviation of the level spacing distribution from the GOE or is it a neccesary condition for GOE(-like) distributions?

The purpose of the present paper is to study some semiclassical consequences of intermittency. Integrable systems may be semiclassically quantized by the WKB method (or rather the EBK method, in cases when the Hamiltonian is non-separable). A more general semiclassical theory is given by the Gutzwiller trace formula [10, 16] where the spectrum is written as a sum over periodic orbits. Successful use of this formula has been made in [17] for an open scattering system fulfilling axiom A, using a simple resummation method. Some progress has recently been made [18–22], applying the trace formula for bound ergodic systems, i.e. bound systems where all periodic orbits are unstable. However, the success in [17] relied heavily on the hyperbolicity, and the associated simple symbolic organization of periodic orbits. Bound chaotic systems are more complicated by, e.g., the presence of intermittency. The symbolic dynamics in an intermittent system is generally infinitely complicated. This is serious because a *simple* symbolic dynamics is crucial for nice analytic properties of the trace formula [23]. This motivates a close study of intermittent properties in realistic bound potentials.

The paper is organized as follows. In the next section we review some semiclassical properties of hyperbolic systems and their relevance to an open system. In section 3 we present a one-parameter family of bound systems which we will use as a strongly intermittent model system and show how this system may be approximately quantized using the WKB method and the adiabatic approximation. In section 4 we derive the action integrals and stability eigenvalues for a family of periodic orbits associated with the intermittent motion. We show how Gutzwiller's trace formula applied to these restricted families provides results which closely resemble the WKB result, but with interesting differences. We round off with a discussion in section 5.

2. Semiclassical mechanics of hyperbolic systems

The semiclassical eigenvalues correspond to the poles of the Gutzwiller trace formula [10, 16] or, equivalently, to the zeros of the Selberg-type zeta function [24], which for systems with two degrees of freedom reads as

$$Z_r(E) = \prod_p \prod_{m=0}^{\infty} \left(1 - t_p \Lambda_p^{-m}\right) \tag{1}$$

where

$$t_p = \chi_{r,p} \frac{\exp(\mathrm{i}[S_p/\hbar - \mu_p \pi/2])}{|\Lambda_p|^{1/2}}. \tag{2}$$

S_p is the action integral for a prime periodic orbit p, Λ_p the expanding eigenvalue of the linearized Poincaré map, and μ_p a geometrical phase index [25]. We have assumed that all orbits are unstable. The quantum eigenstates belong to the irreducible representation (symmetry class) r and the periodic orbits are defined on the fundamental domain (or equivalently in the desymmetrized system). $\chi_{r,p}$ is a symmetry factor [26–28] that depends on the irreducible representation r and the symmetry of the orbit p.

The spectral density function $d(E) \equiv \sum_n \delta(E - E_n)$ is related to the zeta function Z according to

$$d(E) = \bar{d}(E) + \frac{1}{\pi} \operatorname{Im} \frac{\mathrm{d}}{\mathrm{d}E} \ln Z(E) \tag{3}$$

where the energy is assumed to contain a small negative imaginary part. $\bar{d}(E)$ is the mean spectral density.

It is a natural first step to apply equation (1) to axiom-A systems, i.e. systems with a symbolic dynamics, and the stability eigenvalues of all periodic orbits exponentially bounded away from 1. Let us further assume that the symbolic dynamics is binary and *complete*, i.e. each periodic binary code corresponds to one periodic orbit. This is realized, for example, by a symmetric three-disk scattering system, provided the disks are sufficiently separated [17, 29]. The zeta function (1) is dominated by the $m = 0$ factor, Z_0, with expansion [17, 30]

$$Z_0 = 1-t_1-t_0-[t_{10}-t_1t_0]-[t_{100}-t_{10}t_0]-[t_{110}-t_1t_{10}]-[t_{1100}-t_1t_{100}-t_{110}t_0+t_1t_{10}t_0] \\ -[t_{1110}-t_1t_{110}]-[t_{1000}-t_{100}t_0]-\cdots. \quad (4)$$

The expansion is organized in such a way that each square bracket contains some long orbit(s) (length n) minus its approximant(s) in terms of shorter ones. The sizes of these *curvature corrections* fall off exponentially with n. This effect is called *shadowing.* The expansion is dominated by the *fundamental* terms, for example, t_0 and t_1. It was demonstrated in [17] that very accurate results for the quantum resonances can be obtained from (4) by keeping curvature corrections up to some n, and that the results converge rapidly with increasing n.

To get a qualitative idea of what the spectrum looks like, assume that the curvature corrections vanish identically (corresponding to infinitely separated disks) and that $S_1 = S_0 = L \cdot k$ and $\Lambda_1 = \Lambda_0 = \Lambda$, where the wavenumber $k = \sqrt{2E}$ and L is the disk centre separation (we are using units such that $\hbar = m = 1$). The zeta function now approximately equals [31]

$$Z \approx \prod_{m=0}^{\infty} \left(1 - 2\frac{e^{iLk}}{\sqrt{\Lambda}\Lambda^m}\right) \quad (5)$$

with zeros given by

$$k_{n,m} = \frac{2\pi n}{L} - i\left[\lambda\left(\frac{1}{2}+m\right) - h\right] \quad (6)$$

where we have introduced the (average) Liapunov exponent $\lambda = \log\Lambda/L$ and the topological entropy $h = \log 2/L$. The result is a regular lattice of quantum zeros far down in the complex k-plane (remember that the system is open) where the leading quantum resonances correspond to $m = 0$.

The completeness of the symbolic dynamics is crucial for this qualitative result. Suppose that the $\overline{0}$ orbit is pruned (and that for simplicity no other orbit is). (The overline symbol in $\overline{0}$ denotes periodicity, however this symbol will be frequently omitted in the following, since we only refer to *periodic* orbits.) Then there will be a whole sequence of periodic orbits without shadowing terms: $[10^i]$ with $i \geqslant 0$ [30, 31] and these orbits may now be considered as fundamental. It is clear that equation (6) no longer captures the qualitative structure of the spectrum. We will eventually see how intermittency is often associated with such a pruning rule. The associated sequences (like 10^i) which will dominate the expansion of the zeta function will subsequently be called *intermittent sequences* and will have stability eigenvalues typically growing algebraically with i to be compared with the exponential growth in the hyperbolic case.

This will be the case if we close the disk system above. The orbit 0, i.e. the orbit bouncing back and forth between two disks, will thus be pruned. The orbit 10^i will bounce i times in the horn-shaped region where the disks touch. The motion in this region is (asymptotically) integrable and the stability eigenvalues will increase algebraically with i. Note that not only the 0 cycle will be pruned in the closed disk system. In [32] it is argued that there is an infinity of pruning rules and that the pruning may be described in terms of a pruning front [33]. It may very well be the case that an infinite grammar of the symbolic dynamics is a generic property of bound Hamiltonian systems.

3. WKB quantization in the adiabatic approximation

As a model system we will choose the one-parameter family of Hamiltonians

$$H = \tfrac{1}{2}\left(p_x^2 + p_y^2 + (x^2y^2)^{1/a}\right). \tag{7}$$

In the limit $a \to 0$ we obtain the hyperbola billiard. Increasing a means a gradual softening of the billiard walls and when $a = 1$ we recover the frequently studied x^2y^2 potential. The symmetry group of this family is C_{4v}. The periodic orbits in these systems may be described by a symbolic dynamics using a three letter $[2,1,0]$ alphabet [21, 22, 28, 34]. This coding scheme is thoroughly described in [22] together with explicit rules for determining the symmetry factors $\chi_{r,p}$ in terms of the symbol code. The important detail to bear in mind in the subsequent discussion is that a sequence of zeros, as in $\overline{200000} \equiv \overline{20^5}$ corresponds to a number of oscillations in the horn region, see figure 1.

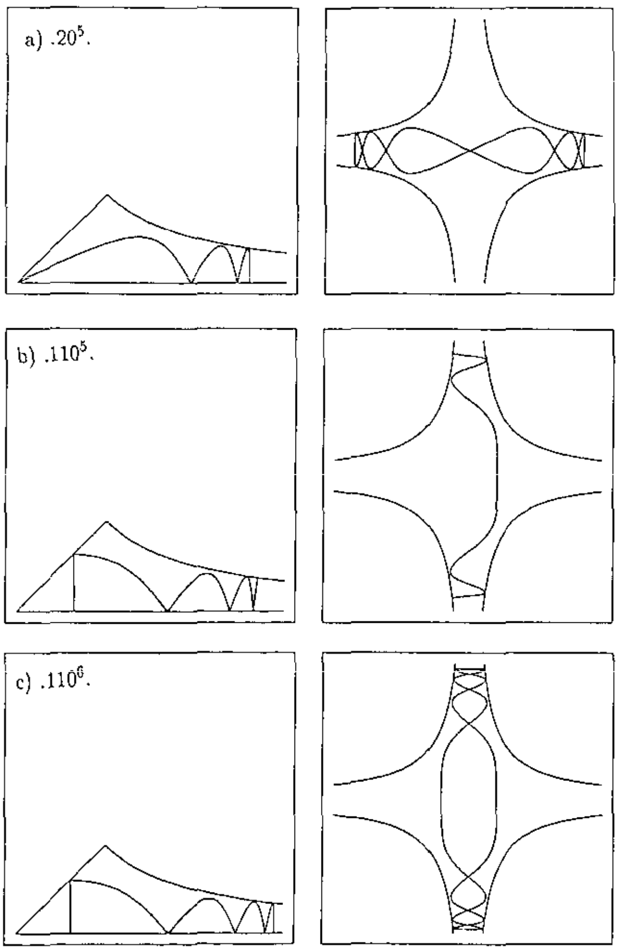

Figure 1. Members of the intermittent sequences 20^i and 110^i, both in the fundamental and full domain. x^2y^2 model

The equipotential curves have horn-shaped regions similar to those in the closed disk systems but now with infinite area; the quantum mechanical spectrum is still discrete. The systems show a typical intermittent behaviour with chaotic scattering in the central region and almost integrable motion out in the horns. The motion in these horn regions may thus be treated in the adiabatic approximation [35] in the following way:

Suppose that $x \gg y$, then the motion in the x direction will be much slower than in the y direction, and x may be regarded as a slowly varying parameter. In the adiabatic approximation the motion in the y direction is described by the Hamiltonian

$$H_y = \tfrac{1}{2}\left(p_y^2 + (x^2y^2)^{1/a}\right). \tag{8}$$

By the adiabatic theorem the action integral in the y direction, as given by

$$J_y = \oint p_y \, \mathrm{d}y = (2H_y)^{(1+a)/2} f(2/a)/x \tag{9}$$

where

$$f(\nu) = \frac{1}{2\pi}\oint \sqrt{1-|z|^\nu}\, \mathrm{d}z \tag{10}$$

is approximately a constant of motion. The full Hamiltonian may now be written as $H \approx \frac{1}{2}p_x^2 + H_y(x)$, giving (approximately) the x motion for any J_y. If we now also transform the (x, p_x) pair to action-angle variables we obtain the following expression for H

$$H \approx \frac{1}{2}\left[J_x J_y \Big/ f\left(\frac{2}{a}\right) f\left(\frac{2}{a+1}\right)\right]^{2/(a+2)}. \tag{11}$$

We note that, although this expression was derived under the (asymmetric) assumption $x \gg y$, the final result is symmetric in x and y. Even though these adiabatic expressions are not valid in the central region it is very tempting to perform a semiclassical quantization of (11). This was indeed done for the special case $a = 1$ in [35]. In the other limit $a \to 0$ (hyperbola billiard) one obtains

$$E_{\mathrm{ad}} = \tfrac{1}{2}\pi(n_x+1)(n_y+1). \tag{12}$$

Note that, in this expression, the factor $(n+1)$ appears and not the more familar factor $(n+\frac{1}{2})$ since reflections off a hard wall acquires a phase shift π, rather than $\pi/2$. Quantum mechanical calculations have been performed for the A_2 representation (denoted by minus signs in the fifth column in table 1) and the B_2 representation (denoted by plus signs) in [36]. These two representations correspond to odd values of (n_x, n_y) since the wavefunctions are odd with respect to the $y = 0$ and $x = 0$ lines. With the two adiabatic states (k, l) and (l, k) one can construct one A_2 and one B_2 state (except the $k = l$ case which always corresponds to a B_2 state). We see from table 1 that the spectrum is surprisingly well described by this simple adiabatic expression. However, due to the central part of the potential where the adiabatic approximation is not applicable, the degeneracy between the two representations is split. Within each representation we clearly see the effect of level repulsion. (The last column in table 1 show averages over the quantum mechanical eigenenergies which should be compared with the (degenerated) semiclassical adiabatic ones in the second column.) Although close to an integrable Hamiltonian, the system is still non-integrable, so this is just what we should expect. Another aspect of this non-integrability is that (almost) all periodic orbits are isolated and unstable. In the strict limit $a \to 0$ all periodic orbits are indeed unstable, but when $a > 0$ small regions in phase space are generally occupied by regular motion [8, 22].

Table 1. Adiabatic and exact quantum eigenvalues in the hyperbola billiard.

n_x	n_y	E_{ad}	E_{QM}		E_{ave}
1	1	6.28	5.87	+	5.87
1	3	12.57	10.73	−	12.20
3	1		13.66	+	
1	5	18.85	18.14	+	18.14
5	1		18.14	−	
1	7	25.13	22.89	+	25.36
3	3		24.71	−	
7	1		28.46	+	
1	9	31.42	29.75	−	30.60
9	1		31.45	+	
1	11	37.70	33.97	−	37.85
3	5		36.81	+	
5	3		38.52	−	
11	1		42.10	+	
1	13	43.98	43.12	−	43.39
13	1		43.67	+	
1	15	50.27	48.27	+	50.34
3	7		48.63	−	
7	3		51.91	+	
15	1		52.56	−	
1	17	56.55	55.10	−	56.60
5	5		55.55	+	
17	1		59.14	+	

The problem of calculating the mean spectral staircase function is similar to the problem of counting the number of integer lattice points below a hyperbola. A solution was given by Dirichlet [37]. The mean number of states below E belonging to representation A_2 and B_2 is then found to be (cf appendix)

$$\bar{N}_{\text{adiab}}(E) = \frac{E}{2\pi}\ln(E) + \frac{E}{2\pi}[2\gamma - 1 - \ln(2\pi)] + \mathrm{o}(\sqrt{E}). \tag{13}$$

This expression should be compared with the result of [38]

$$\overline{N}(E) = \frac{E}{2\pi}\ln(E) + \frac{E}{2\pi}[2\gamma + \ln(2) - 2\ln(2\pi)] + \mathrm{o}(\sqrt{E}). \tag{14}$$

The adiabatic expression is obtained from an extrapolation into the region where the adiabatic approximation is not valid whereas the latter formula is the result of a careful analysis of the central region as well as the arms. The results only differ by 10% in the second term.

4. Periodic orbit quantization in the adiabatic approximation

The aim of this section is to see to what extent we can reproduce the WKB result of the last section by means of periodic orbit theory. There are two families of periodic orbits exploring only the arms of the potentials (7) and which may be relevant for this purpose. These are the infinite sequences 20^i and 110^i, cf figure 1. These orbits may be considered as fundamental since they cannot be pieced together from shorter orbits because of the pruning of the zero cycle. We can now write down an approximation of the zeta function by means of a sum over the fundamental orbits, cf equation (4), only taking into account orbits exclusively exploring the arms

$$Z_{\mathrm{ad}}(E) \approx 1 - \sum_{p=20^i} t_p - \sum_{p=110^i} t_p \tag{15}$$

where t_p is given by equation (2). It is a poor approximation of the full zeta fucntion, since it neglects the influence of the central chaotic region, but it is likely to be related to the WKB result of the previous section. In (15) we have omitted the factors in equations (1) with $m > 0$.

Our objective now is to calculate the S_p and Λ_p for intermittent sequences such as 20^i. We will also (for the moment) restrict ourselves to the special case $a \to 0$, where we have the adiabatic Hamiltonian (cf (11))

$$H = \tfrac{1}{2}\pi J_x J_y . \tag{16}$$

From the fundamental relation $\omega = \partial H/\partial J$ we get

$$\begin{cases} \omega_x = \frac{1}{2}\pi J_y \\ \omega_y = \frac{1}{2}\pi J_x . \end{cases} \tag{17}$$

An orbit in the family 20^i makes $(i+1)/2$ full oscillations in the y direction for each 1/2 oscillation in the x direction (this corresponds to one traversal of the periodic orbit in the fundamental domain, but only half of the corresponding periodic orbit in the full domain, cf figures 1 and 2):

$$\frac{\omega_y}{\omega_x} = \frac{J_x}{J_y} = i + 1 . \tag{18}$$

Equating (16) and (17) gives J_x and J_y so that we may express the total action integral S_p as

$$S_p = 2\pi(\tfrac{1}{2}J_x + \tfrac{1}{2}(i+1)J_y) = \sqrt{4\pi(i+1)}\, k(E) \tag{19}$$

where $k(E) = \sqrt{2E}$ is the momentum (or wavenumber).

The stability is slightly more complicated to calculate. To this end we introduce the Poincaré surface of section $y = 0$, thus defining the area-preserving map $(x', p'_x) \mapsto (x'', p''_x)$ The aim is to calculate the stability (or monodromy) matrix M

$$M = \begin{pmatrix} \partial x''/\partial x' & \partial x''/\partial \dot{x}' \\ \partial \dot{x}''/\partial x' & \partial \dot{x}''/\partial \dot{x}' \end{pmatrix} . \tag{20}$$

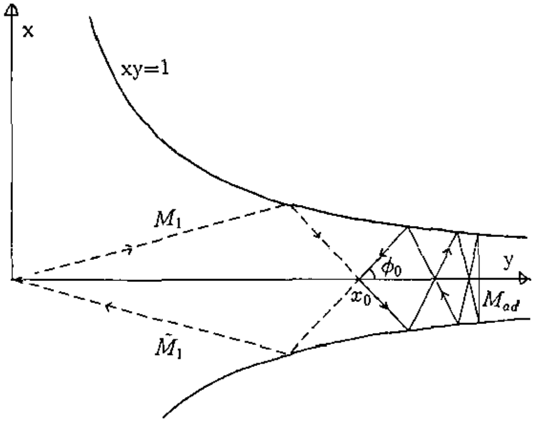

Figure 2. The stability matrix M is factorized as $M = \tilde{M}_1 M_{ad} M_1$ where M_{ad} is calculated in the adiabatic approximation.

The adiabatic approximation breaks down in the central region. The results in the previous paragraph for the action integral could, however, be continued into this region without trouble. This is not possible when calculating the stability. In order to calculate the stability for the orbits 20' we split the orbit into three parts according to figure 2 and write $M = \tilde{M}_1 M_{ad} M_1$ where only M_{ad} is to be calculated in the adiabatic approximation.

The idea now is to introduce variations $\delta x'$ and $\delta p'_x$ and write down adiabatic equations to determine $\delta x''$ and $\delta p''_x$ uniquely. We are also going to restrict ourselves to orbits starting and ending at $x' = x'' = x_0$ with momentum $p'_x = -p''_x = k\cos(\phi_0)$. Without loss of generality we can set $k(E) = \sqrt{2E} = 1$. To this end we rewrite equation (9) as $(a = 0)$

$$H_y = \tfrac{1}{8}\pi^2 J_y^2 x^2. \tag{21}$$

Conservation of energy gives

$$E = \tfrac{1}{2}p_x^2 + H_y(x). \tag{22}$$

We can now write down the total phase traversed in the y direction

$$F(x', x'', J_y) = \int \frac{\omega_y}{p_x}\,\mathrm{d}x = \oint_{x'}^{x''} \frac{\pi^2}{4} \frac{J_y x^2\,\mathrm{d}x}{\sqrt{1 - \frac{1}{4}\pi^2 J_y^2 x^2}} = N_y \pi \tag{23}$$

which is an integer multiple of π. Due to the definition of the Poincaré section, F will remain constant when varying x' and p'_x, so that the requested set of equations equations becomes

$$\begin{aligned} &\delta F(x', x'', J_y) = 0 \\ &p_x'^2 + \tfrac{1}{4}\pi^2 J_y^2 x'^2 = 1 \\ &p_x''^2 + \tfrac{1}{4}\pi^2 J_y^2 x''^2 = 1. \end{aligned} \tag{24}$$

If, for example, we vary x' but keep $\delta p'_x = 0$, it is straightforward to calculate $\delta x''$ and $\delta p''_x$. We arrive at

$$M_{\rm ad} = \begin{pmatrix} 1+\frac{s}{c^3}f & \frac{2}{\pi J_y}\frac{s^2}{c^4}\left(f+\frac{c^3}{s}\right) \\ \frac{\pi J_y}{2}\frac{f}{c^2} & 1+\frac{s}{c^3}f \end{pmatrix} \tag{25}$$

where

$$s=\sin(\phi_0) \qquad c=\cos(\phi_0) \qquad f=\sin(2\phi_0)+2\phi_0. \tag{26}$$

M_1 is obtained from simple geometric considerations. We cite the results obtained in the limit $\phi_0 \ll 1$, corresponding to $i \gg 0$ in 20^i

$$M_1 = \begin{pmatrix} \frac{5}{9} & \frac{2}{3}\phi_0^{-5/2} \\ 6\phi_0^{5/2} & 9 \end{pmatrix}. \tag{27}$$

$\tilde{M}_1$ is obtained from time-reversal symmetry

$$\tilde{M}_1 = \begin{pmatrix} 1 & 0 \\ 0 & -1 \end{pmatrix} M_1^{-1} \begin{pmatrix} 1 & 0 \\ 0 & -1 \end{pmatrix} = \begin{pmatrix} M_{1,22} & M_{1,12} \\ M_{1,21} & M_{1,11} \end{pmatrix}. \tag{28}$$

Taking the limit $\phi_0 \ll 1$ in (25), multiplying $M = \tilde{M}_1 M_{\rm ad} M_1$, and taking the trace gives

$$\mathrm{Tr}(M) = \frac{39\pi}{\phi_0^3}. \tag{29}$$

All that remains is to relate the angle ϕ_0 to the number i in 20^i. Simple geometry relates $x'' = x' \equiv x_0$ with ϕ_0

$$x_0 \approx \frac{4}{\sqrt{3\phi_0}}. \tag{30}$$

Since $p'_x = \cos(\phi_0)$ (remember $k(E)=1$) and through (24) we have

$$\tfrac{1}{2}\pi J_y x_0 = \sin(\phi_0) \approx \phi_0. \tag{31}$$

These two expressions thus relate ϕ_0 to the adiabatic invariant J_y. Through (16) and (18) we have a relation between J_y and i. We thus arrive at

$$\mathrm{Tr}(M) = \tfrac{117}{4}(i+1). \tag{32}$$

The result is an asymptotic linear increase in the stability eigenvalues with i. Comparison between the result of (19) and (32) with numerical results are displayed

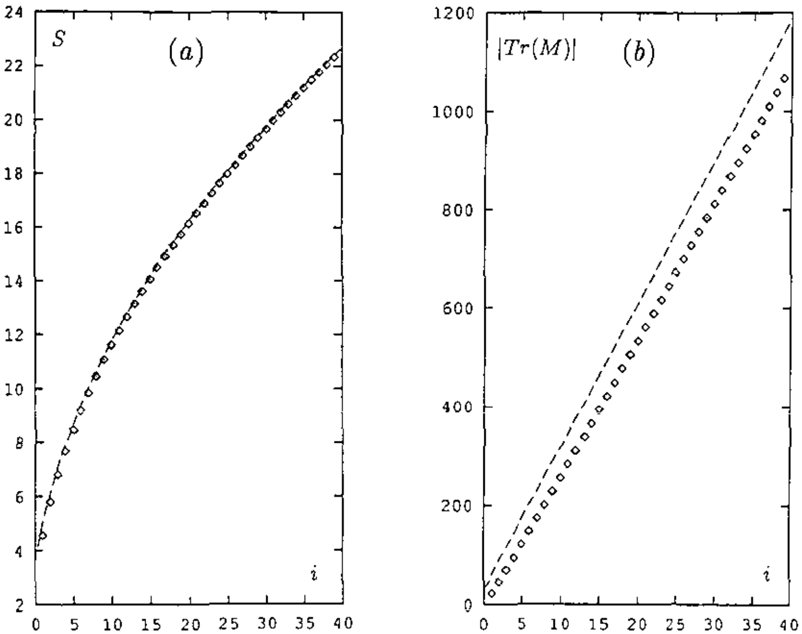

Figure 3. Action integrals (*a*) and the trace of the stability matrix (*b*) calculated in the adiabatic approximation (broken curve) and numerically (squares), for the sequence 20^i in the hyperbola billiard, $k(E) = 1$.

in figure 3. The actions $S(k)$ agree extremely well. The slope of the traces approach the calculated value of 117/4 but there is a small shift.

The associated Liapunov exponents tend to zero

$$\lambda_i = \frac{\log \Lambda_i}{T_i} \sim \frac{\log i}{\sqrt{i}} \to 0 \qquad i \to \infty \tag{33}$$

which, as we have said, is typical for an intermittent system.

A similar treatment may be given to the intermittent sequence 110^i. The result is still a linear increase in $\mathrm{Tr}(M)$ but with a much larger prefactor. The last sum in (15) may thus be omitted. To write down the adiabatic zeta function we only need the symmetry factors $\chi_{r,p}$ and the phase indices μ_p. From the expressions in (22) we obtain

$$\begin{aligned} \chi_{r,p} &= (-1)^i \qquad \text{if } r = A_2, B_2 \\ \mu_p &= 2(i+1). \end{aligned} \tag{34}$$

We can now write down the adiabatic zeta function Z_{ad} as

$$Z_{\mathrm{ad}} \equiv 1 - \sum_{p=20^i} t_p \approx 1 + c \sum_{j=1}^{\infty} \frac{\exp(\mathrm{i}\sqrt{4\pi j}\, k(E))}{\sqrt{j}} \tag{35}$$

where

$$c = \sqrt{\tfrac{4}{117}} \approx 0.185 \qquad a = 0. \tag{36}$$

A similar calculation for the x^2y^2 model, that is $a = 1$, also yields a linear increase in $\mathrm{Tr}(M)$ for both the intermittent sequences. The calculation in the central region is more difficult to make accurately but numerically one finds that the slopes of $\mathrm{Tr}(M)$ against i are 24.6 and 23.5 for the 20^i and 110^i sequences, respectively. The adiabatic zeta function for the $a = 1$ case is thus given by (35) but with $c \approx 0.41$, and with a simple rescaling of energy.

It would now be interesting to study the staircase function

$$N_{\mathrm{ad}}(E) - \bar{N}(E) \equiv \frac{2}{\pi}\,\mathrm{Im}\log Z_{\mathrm{ad}}(E) \qquad r = A_2 + B_2 \tag{37}$$

and to compare it with the corresponding WKB result: $N_{\mathrm{WKB}}(E) - \bar{N}(E)$, where $N_{\mathrm{WKB}}(E)$ is obtained from (12) and $\bar{N}(E)$ is given by (14).

The series in (37) converges absolutely if $\mathrm{Im}(E) > 0$ and diverges if $\mathrm{Im}(E) < 0$. However when $\mathrm{Im}(E) = 0$, expression (37) seems to converge and the result obtained from the first 100 terms is displayed in figures 4(a) and (c).

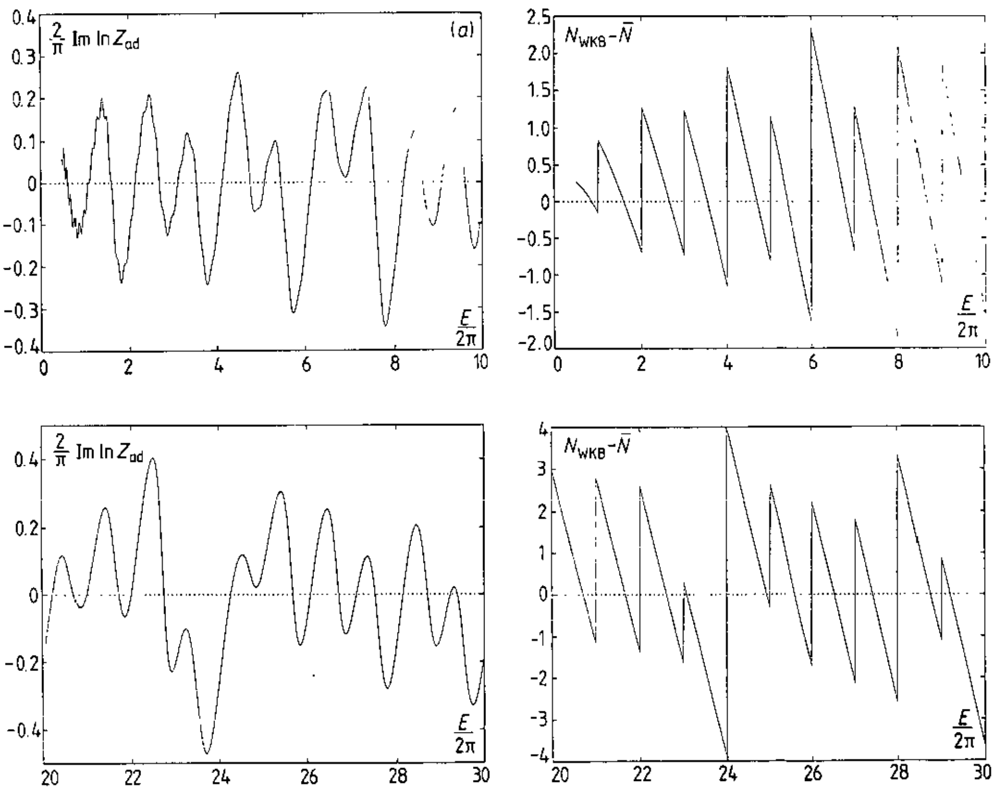

Figure 4. Spectral staircase function calculated in the adiabatic approximation using periodic orbit theory ((a) and (c)) and the WKB method ((b) and (d)).

The corresponding WKB result may be seen in figures 4(b) and (d). We note a striking similarity. The intermittent sequences yield peaks close to the WKB positions and there is a clear correlation between the degeneracy of the WKB eigenvalues and the height of the peaks in figures 4(a) and 4(c). Clearly the periodic orbit result is smeared out compared with the WKB one. However, the most important difference between the two figures is the amplitude of the oscillations. Clearly, the periodic orbits that went into this calculation only constitute a small subset. Therefore they will not, by themselves, produce zeros on or close to the real k axis of the corresponding zeta function. The result from this adiabatic calculation should be interpreted instead as an integrable component of the spectrum. However, not in the sense of [14] where certain levels (in the semiclassical limit) are associated with regular motion and some with irregular motion. For finite energies it will be recognizable as a tendency of the spectrum towards the integrable result of equation (12).

In the $a = 1$ case the only difference lies in the factor c which is larger; the result is quite similar to those in figures 4(a) and (c) but with roughly twice the amplitude.

5. Discussion

It is instructive at this point to review an expansion of the full zeta function (1) that was made in [22] for the hyperbola billiard. The zeta function is then written as a sum over all possible linear combinations $n = [m_p]$,

$$Z(E) = \sum_n C_n \mathrm{e}^{\mathrm{i}[S_n - \mu_n \pi/2]} \tag{38}$$

where we have defined the quantities

$$S_n = \sum_p m_p S_p \tag{39}$$

$$\mu_n = \sum_p m_p \mu_p . \tag{40}$$

The C_n are amplitudes related to the stability eigenvalues. In [22] this series was ordered according to decreasing amplitudes. The first 100 terms for hyperbola billiard in the A_2 representation are given in table 2. We use the obvious notation

$$Z = \sum_n [(-1)^{m_{p_1}} t_{p_1}^{m_{p_1}}][(-1)^{m_{p_2}} t_{p_2}^{m_{p_2}}] \ldots . \tag{41}$$

The (infinite number of) factors with $m = 0$ are omitted from the table since $t_p^{m=0} = 1$.

We note that there are no terms with $m > 1$ among the first 100 pseudo orbits so this justifies the omission of all higher factors in (1).

We also made the shadowing assumption, but terms like $t_{2002000} - t_{200} t_{2000}$ are not very abundant in the expansion and the cancellation works pretty well.

The series is dominated by two types of intermittent sequences and cross terms among them. First there are the infinite ones, already discussed: 110^i and 20^i, this subset of the expansion is well approximated by (35). Then there are finite sequences exploring both the central region and the arms. Example of this latter kind are 10^i, 21210^i and 220^i terminating at $i = 5$, 16 and 51, respectively. These are not fundamental in the sense of [30], since they may, in some sense, be approximated by shorter orbits exploring only the central and horn regions, respectively. However,

Table 2. Expansion of the Selberg zeta function. Hyperbola billiard in the A_2 representation.

1	1	26	$-t_{1000}$	51	$-t_{2110}$	76	$-t_{220^{11}}$
2	$-t_1$	27	$-t_{20^7}$	52	$-t_{1000}$	77	$-t_{2210^4}$
3	$-t_{21}$	28	$-t_{1100}$	53	$-t_{2121000}$	78	$-t_{21210^8}$
4	$-t_{210}$	29	$-t_2$	54	$t_{21}t_{10}$	79	$-t_{220^{12}}$
5	$-t_{2100}$	30	$-t_{22000}$	55	$-t_{220^7}$	80	$-t_{20^{16}}$
6	$-t_{21000}$	31	$t_{21}t_{2100}$	56	$-t_{20^{12}}$	81	$t_{20}t_{21000}$
7	$-t_{20}$	32	$-t_{2210}$	57	$-t_{2120}$	82	$-t_{21210^9}$
8	$-t_{10}$	33	t_1t_{20}	58	$-t_{21210^4}$	83	$-t_{220^{13}}$
9	$-t_{200}$	34	$t_{21}t_{21000}$	59	$-t_{220^8}$	84	$-t_{10^4}$
10	$-t_{2000}$	35	$-t_{20^8}$	60	$-t_{221000}$	85	$t_{10}t_{2100}$
11	$-t_{100}$	36	t_1t_{10}	61	$-t_{20^{13}}$	86	$-t_{2121 0^{10}}$
12	t_1t_{21}	37	$-t_{220^4}$	62	$-t_{21210^5}$	87	$-t_{20^{17}}$
13	$-t_{220}$	38	$-t_{21210}$	63	$t_{20}t_{210}$	88	$-t_{220^{14}}$
14	$-t_{20^4}$	39	$-t_{20^9}$	64	$-t_{220^9}$	89	$-t_{21210^{11}}$
15	$-t_{110}$	40	$t_{210}t_{2100}$	65	$-t_{20^{14}}$	90	$-t_{110^5}$
16	$-t_{221}$	41	$-t_{220^5}$	66	$-t_{110^4}$	91	$t_{10}t_{21000}$
17	t_1t_{210}	42	$-t_{20^{10}}$	67	t_1t_{200}	92	$-t_{21210^{12}}$
18	$-t_{20^5}$	43	$t_{210}t_{21000}$	68	$-t_{21210^6}$	93	$-t_{2210^5}$
19	$-t_{211}$	44	$-t_{22100}$	69	$-t_{220^{10}}$	94	$-t_{220^{15}}$
20	t_1t_{2100}	45	$-t_{212100}$	70	$-t_{1020}$	95	$-t_{20^{18}}$
21	t_1t_{21000}	46	$t_{21}t_{20}$	71	$-t_{1200}$	96	$-t_{21210^{13}}$
22	$-t_{2200}$	47	$-t_{11000}$	72	$-t_{21210^7}$	97	$-t_{220^{16}}$
23	$-t_{120}$	48	$-t_{220^6}$	73	$t_{10}t_{210}$	98	$-t_{21100}$
24	$-t_{20^6}$	49	$-t_{20^{11}}$	74	$-t_{20^{15}}$	99	$-t_{12100}$
25	$t_{21}t_{210}$	50	$t_{2100}t_{21000}$	75	$t_{20}t_{2100}$	100	$-t_{21210^{14}}$

no straightforward shadowing scheme has been worked out for the hyperbola billiard and a simple inspection of table 2 does not indicate any effective shadowing among long orbits and combinations of shorter ones. The finite intermittent sequences *are* of fundamental importance in the expansion of the zeta function, representing the coupling between the central chaotic region and the intermittent horns. The traces of the stability matrix $\mathrm{Tr}(M)$ for the finite sequences increases slower than linearly with the number of zeros, as seen in figure 5(a).

In [19, 22, 39] it was demonstrated that the cycle expansions, such as equation (38) yields zeros close to the real k axis, where there is a one-to-one correspondence between the real part of the zeros and the quantum mechanical eigenenergies, at least for low energies.

For the case treated earlier the infinite intermittent sequences, associated with an integrable spectrum, and the finite sequences, representing the coupling with the central stochastic region of the potential, should cooperate in order to produce these zeros. These zeros exhibit level repulsion compared with the underlying integrable result, see table 1.

In the x^2y^2 model the sequences 10^i and 220^i already terminate at $i = 0$ and 7, respectively. We also noted that the amplitude of the phase variations of Z_{ad} was twice as large as those in the hyperbola billiard. The adiabatic+WKB result of [35] (corresponding to equation (12)) also agreed better with the exact quantum mechanical result.

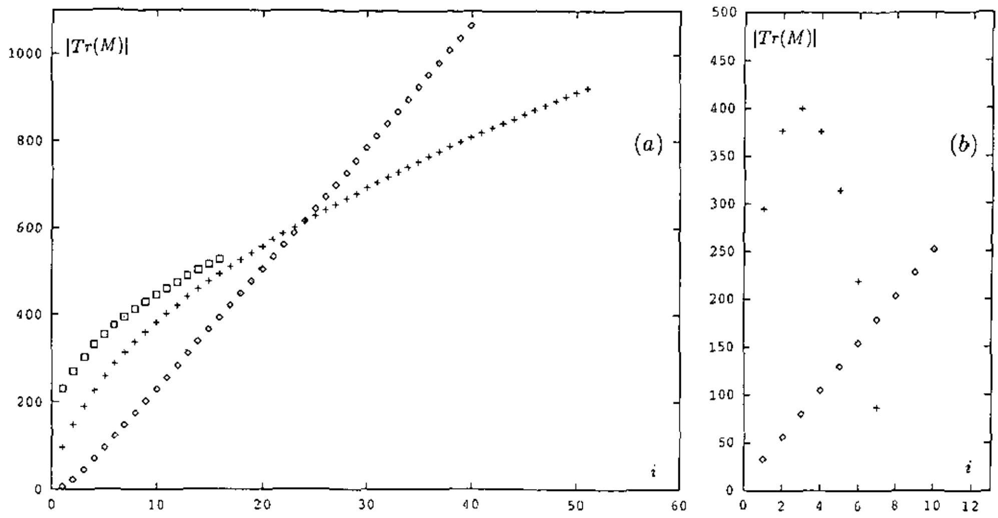

Figure 5. (*a*) The trace of the stability matrix for the infinite sequence 20^i (◇) and the finite sequences 21210^i (+) and 220^i (□) for the hyperbola billiard. (*b*) The trace of the stability matrix for the infinite sequence 20^i (◇) and the finite sequence 220^i (□) for the x^2y^2 model.

In the smooth systems $a > 0$, $\mathrm{Tr}(M)$ will, in the general case, not even increase monotonically with the number of 0 in the code. This is illustrated by the sequence 220^i in the x^2y^2 model in figure 5(*b*). The reason is that when a periodic orbit is pruned through a bifurcation, its stability eigenvalue has to be unity. When the parameter a is increased from 0 to 1 the associated curve in figure 5(*a*) will bend down and members of the sequence 220^k will be pruned one by one [22]. In a small range in the parameter a there will be a stable island surrounding the orbit which is about to be pruned. The presence of stable orbit induces divergences in the trace formula.

Even if we were so lucky that no stable islands exist for the parameter value we have happened to choose, it is evident that these effects will cause serious problems in any attempt to apply the trace formula. A regularization scheme based on an analogy of the Riemann–Siegel formula [18] will clearly not capture such an intricate structure in the sequences of cycle invariants, which we must expect to find in any simple smooth bound system one uses to model chaos. We are thus far from any *simple* rules for quantizing chaos.

The potentials treated in this paper are special in the sense that the phase space associated with the intermittent motion is infinite. The extent to which the wavefunctions penetrate the horn regions is given by the de Broglie wavelength. But as the energy tends to infinity the ratio between the area of the accessible horn region and the central region increases. The question is whether the energy spectrum is described more accurately by (12), as the energy increases. In particular adiabatic states with $n_x \gg n_y$ and $n_y \gg n_x$ should give an accurate description, see [40, 41]. The published eigenvalues in the hyperbola billiard are too few to give any hints of the tendency.

In [36] it is argued that the level spacing distribution in the hyperbola billiard is given by (or similar to) GOE, but the number of obtained eigenstates is too low

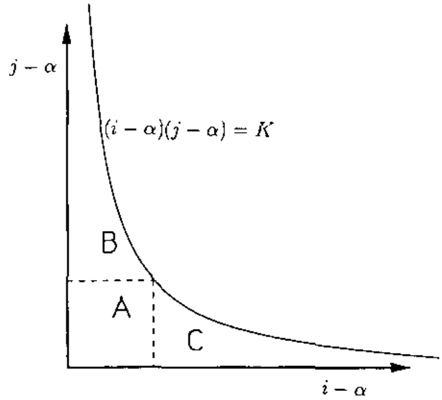

Figure 6. The region under the hyperbola is divided into three subregions.

to provide a significant result. The question is whether the integrable tendency represented by the intermittent subregions of phase space is a necessary component to obtain a GOE-like level spacing distribution or whether it will mean deviations from GOE. Studies of the stadium billiard suggests the latter possibility [42]. The marginally stable orbit between the straight sections corresponds to an underlying integrable component of the spectrum in very much the same way as the result earlier and it is argued that this will induce an increased probability of occasional degeneracies compared with GOE.

Usually the spectral rigidity deviates significantly from the predictions of [43], where the spectral rigidity is predicted to agree with GOE up to a certain breakpoint related to the shortest periodic orbit in the system. Such deviations are reported in [12, 13, 44] for the anisotropic Kepler problem, Sinai's billiard and the hyperbola billiard respectively. If a system is intermittent, as, for example, Sinai's billiard, the time scale relevant for this breakpoint should naturally be associated with the intermittency rather than the shortest periodic orbit in the system. The anisotropic Kepler problem in [12] is characterized by a phase space densely filled by cantori [45] and an extreme type of intermittency; there are families of periodic orbits, associated with the collision manifolds, with accumulating eigenvalues [39], which should be compared with the algebraically increasing eigenvalues in this article. In [46] it is demonstrated how transport barriers, such as island chains and cantori, induce deviations from the GOE for finite energies (thus not in the strict semiclassical limit). It should be noted that cantori may exist even in chaotic billiards [47]. These examples show how timescales, for example, due to barriers, short periodic orbits and intermittency, naturally give bounds to a possible universal regime. It has been stressed in the present paper that such features may not be avoided in chaotic systems. Low-dimensional chaotic systems show a rich and varying behaviour, leaving traces in the spectral measures. It is a challenge for the future to understand the subtle interplay between features such as cantori, intermittency, stable islands on the quantum level as well as localization effects of the wavefunctions.

Acknowledgments

I would like to thank S Creagh, P Cvitanović and G Russberg for fruitful discussions.

Appendix

In this appendix we slightly generalize a result due to Dirichlet [37] which we need in order to calculate the mean level staircase $\bar{N}(E)$ for systems where the energy levels are given by

$$K(E) = (i-\alpha)(j-\alpha) \tag{42}$$

where i and j are positive integers and $0 \leqslant \alpha < 1$. We therefore ask ourselves: how many integer pairs (i,j) are there such that $(i-\alpha)(j-\alpha) < K$. We call this number N and, with the notations in figure 6, we can write

$$N(K) = 2N_{A+B} - N_A = 2 \sum_{\substack{0\leqslant i-\alpha\leqslant\sqrt{K} \\ 0\leqslant(i-\alpha)(j-\alpha)\leqslant K}} - \left(\sum_{0\leqslant i-\alpha\leqslant\sqrt{K}}\right)\left(\sum_{0\leqslant j-\alpha\leqslant\sqrt{K}}\right) \tag{43}$$

$$= 2 \sum_{0\leqslant i-\alpha\leqslant\sqrt{K}} \left[\frac{K}{i-\alpha} + \alpha\right] - [\sqrt{K} + \alpha]^2 \tag{44}$$

where [ ] denotes *integral fraction of.* It is now straightforward to show

$$N(E) = 2K \sum_{i=1}^{[\sqrt{K}-\alpha]} \frac{1}{i-\alpha} - K + \mathrm{O}(\sqrt{K}). \tag{45}$$

We now need to calculate a sum such as $\sum_{i=1}^{N} 1/(i-\alpha)$. To that end we expand the terms in the sum to a geometric series. Exchanging the order of summation we get

$$\sum_{i=1}^{N} \frac{1}{i-\alpha} = \sum_{k=0}^{\infty}\sum_{i=1}^{N} \frac{\alpha^k}{i^{k+1}} = \ln(N) + \gamma + \sum_{k=1}^{\infty} \alpha^k \zeta(k+1) + \mathrm{O}\left(\frac{1}{N}\right) \tag{46}$$

where γ is Euler's constant and ζ the Riemann zeta function. Introducing the constants

$$\gamma_\alpha = \gamma + \sum_{k=1}^{\infty} \alpha^k \zeta(k+1) \tag{47}$$

we can write down our final mean level staircase as

$$\bar{N}(K) = K\ln(K) + (2\gamma_\alpha - 1)K + \mathrm{O}(\sqrt{K}). \tag{48}$$

Example. Let us demonstrate how to use this result to estimate the mean spectral staircase for a system with eigenenergies given by

$$E = \tfrac{1}{2}\pi(n_x+1)(n_y+1) \tag{49}$$

in the representations $A_2 + B_2$. The quantum number are thus odd: $n_x = 2i - 1$ and $n_y = 2j - 1$, where i and j are positive integers. The function $K(E)$ in (42) is $K(E) = E/2\pi$ and $\alpha = 0$. The result is given in equation (37).

Non-zero α appears in other representations and/or other phase indices.

References

[1] Greene J M 1968 *J. Math. Phys.* **9** 760; 1979 *J. Math. Phys.* **20** 1183
[2] Bunimovich L A 1974 *Function Anal. Appl.* **8** 254; 1979 *Commun. Math. Phys.* **65** 295
[3] Vivaldi F, Casati G and Guarneri I 1983 *Phys. Rev. Lett.* **51** 727
[4] Sinai Y G 1970 *Russ. Math. Surv.* **25** 137
[5] Arnold V I and Avez A 1968 *Ergodic Problems of Classical Mechanics* (New York: Benjamin)
[6] Donnay and Liveriani 1991 *Commun. Math. Phys.* **135** 267
[7] Machta J and Reinhold B 1986 *J. Stat. Phys.* **42** 949
[8] Dahlqvist P and Russberg G 1990 *Phys. Rev. Lett.* **65** 2837
[9] Karney C F F 1983 *Physica* D **8** 360
[10] Gutzwiller M C 1990 *Chaos in Classical and Quantum Mechanics* (New York: Springer)
[11] Bohigas O, Giannoni M J and Schmit C 1984 *Phys. Rev. Lett.* **52** 1
[12] Wintgen D, Marxer H and Briggs J S 1988 *Phys. Rev. Lett.* **61** 1803
[13] Arve P 1991 *Phys. Rev.* A **44** 6920
[14] Percival I C 1973 *J. Phys. B: At. Mol. Phys.* **6** L229
[15] Bohigas O, Tomsovic S and Ullmo D 1990 *Phys. Rev. Lett.* **64** 1479
[16] Gutzwiller M C 1967 *J. Math. Phys.* **8** 197; 1969 *J. Math. Phys.* **10** 1004; 1970 *J. Math. Phys.* **11** 1791
[17] Cvitanović P and Eckhardt B 1989 *Phys. Rev. Lett.* **63** 823
[18] Berry M V and Keating J P 1990 *J. Phys. A: Math. Gen.* **23** 4839
[19] Tanner G, Scherer B, Bogomolny E B, Eckhardt B and Wintgen D 1991 *Phys. Rev. Lett.* **67** 2410
[20] Bogomolny E B 1992 *Chaos* **2** 5
[21] Sieber M and Steiner F 1991 *Phys. Rev. Lett.* **67** 1941
[22] Dahlqvist P and Russberg G 1991 *J. Phys. A: Math. Gen.* **24** 4763
[23] Cvitanović P 1992 *Chaos* **2** 1
[24] Voros A 1988 *J. Phys. A: Math. Gen.* **21** 685
[25] Creagh S, Robbins J and Littlejohn R 1990 *Phys. Rev.* A **42** 1907
[26] Robbins J 1989 *Phys. Rev.* A **40** 2128
[27] Lauritzen B 1991 *Phys. Rev.* A **43** 603
[28] Cvitanović P and Eckhardt B 1992 Symmetry decomposition of chaotic dynamics *Nonlinearity* at press
[29] Gaspard P and Rice S A 1989 *J. Chem. Phys.* **90** 2225
[30] Artuso R, Aurell E and Cvitanović P 1990 *Nonlinearity* **3** 325, 361
[31] Cvitanović P 1991 *Applications of Chaos (Electrical Power Research Institute workshop 1990)* ed J H Kim and J Stringer (New York: Wiley)
[32] Hansen K 1991 *Chaos* **2** 71
[33] Cvitanović P *(Proc. Los Alamos Center for Nonlinear Science, Nonlinear Science—Next Decade, May 1990) Physica* D **51** 138
[34] Christiansen F 1989 Analysis of chaotic dynamical systems in terms of cycles *Master Thesis* Niels Bohr Institute, University of Copenhagen
[35] Martens C C, Waterland R L and Reinhardt W P 1989 *J. Chem. Phys.* **90** 2328
[36] Sieber M and Steiner F 1990 *Physica* D **44** 248; 1990 *Phys. Lett.* **148A** 415
[37] Rademacher H *Lectures on Elementary Number Theory* (New York: Blaisdell)
[38] Steiner F and Trillenberg P 1990 *J. Math. Phys.* **31** 1670
[39] Christiansen F and Cvitanović P 1992 *Chaos* **2**
[40] Zakrzewski J and Marcinek R 1990 *Phys. Rev.* A **42** 7172
[41] Eckhardt B, Hose G and Pollak E 1989 *Phys. Rev.* A **39** 3776
[42] Creagh S and Littlejohn R unpublished
[43] Berry M V 1985 *Proc. R. Soc.* A **400** 229
[44] Sieber M 1991 The hyperbola billiard: a model for semiclassical quantization of chaotic systems *Thesis* Hamburg
[45] Mackay R S, Meiss J D and Percival I C 1984 *Physica* D **13** 55
[46] Bohigas O, Tomsovic S and Ullmo D 1990 *Phys. Rev. Lett.* **65** 5
[47] Meiss J D 1992 *Quantum Chaos–Quantum Measurement (NATO Advanced Research Workshop 1991)* ed P Cvitanović, I Percival and A Wirzba (Dordrecht: Kluwer)